

# The Influence of Molasses Concentration on the Physical and Mechanical Properties of Evaporation Boat Waste-Based Crucibles

Rusiyanto Rusiyanto<sup>1\*</sup>, Rahmat Doni Widodo<sup>1</sup>, Ares Yudi Prasetyo<sup>1</sup>, Deni Fajar Fitriyana<sup>1\*</sup>, Aldias Bahatmaka<sup>1</sup>, Sudyono Sudyono<sup>1</sup>, Rizki Setiadi<sup>1</sup>, Wara Dyah Pita Rengga<sup>2</sup>, Rifky Ismail<sup>3</sup>, Athanasius Priharyoto Bayuseno<sup>3</sup>, Anjar Priyatmojo<sup>4</sup>, Wahyu Ramdhani<sup>5</sup>, Ferry arifiadi<sup>6</sup>, Chusni Ansori<sup>7</sup>, Agustinus Purna Irawan<sup>8</sup>, Tezara Cionita<sup>9</sup>, Januar Parlaungan Siregar<sup>10</sup>

<sup>1</sup> Department of Mechanical Engineering, Faculty of Engineering, Universitas Negeri Semarang, Semarang 50229, INDONESIA

<sup>2</sup> Department of Chemical Engineering, Faculty of Engineering, Universitas Negeri Semarang, Semarang 50229, INDONESIA

<sup>3</sup> Department of Mechanical Engineering, Faculty of Engineering, Diponegoro University, Semarang 50275, INDONESIA

<sup>4</sup> Material Science and Technology, Faculty of Engineering, Institut Teknologi Bandung, Bandung 40132, INDONESIA

<sup>5</sup> National Research and Innovation Agency, Republic of Indonesia, Bandung 40173, INDONESIA

<sup>6</sup> Balai Besar Keramik, The Industrial Research and Development Agency, Ministry of Industry, Republic of Indonesia, Bandung 40272, INDONESIA

<sup>7</sup> Geological Resources Research Centre, National Research and Innovation Agency, Republic of Indonesia, Bandung 40135, INDONESIA

<sup>8</sup> Faculty of Engineering, Universitas Tarumanagara, Jakarta Barat 11440, INDONESIA

<sup>9</sup> Faculty of Engineering and Quantity Surveying, INTI International University, Nilai 71800, Negeri Sembilan, MALAYSIA

<sup>10</sup> Faculty of Mechanical & Automotive Engineering Technology, Universiti Malaysia Pahang Al-Sultan Abdullah, Pekan 26600, Pahang, MALAYSIA

\*Corresponding Author: [me\\_rusiyanto@unnes.ac.id](mailto:me_rusiyanto@unnes.ac.id), [deniifa89@mail.unnes.ac.id](mailto:deniifa89@mail.unnes.ac.id)

DOI: <https://doi.org/10.30880/ijie.2024.16.01.005>

## Article Info

Received: 12 December 2023

Accepted: 9 March 2024

Available online: 25 April 2024

## Keywords

Crucible, evaporation boat waste, molasses, mechanical and physical properties

## Abstract

Crucibles are critical equipment utilized across numerous industries, and they are notably costly. In this study, the influence of molasses concentrations on the properties of crucibles fabricated from evaporation boat waste products is explored. The evaporation boat waste was powdered and filtered using a 100 mesh sieve. The molasses concentrations added during the mixing procedure were as follows: 0%, 5%, 10%, 15%, and 20% by weight. After 120 minutes, the mixture was compacted using 25 MPa pressure. The green body formed was dried at 100°C for 300 minutes and fired at 1150°C for 240 minutes. The obtained specimens were analyzed by X-ray diffraction (XRD), scanning electron microscopy (SEM), density testing, hardness testing, and flexural testing. The results of this study demonstrate that the addition of molasses has significant effects on the properties of the crucibles.

Specimens using molasses with a concentration of 5 wt% produce better physical and mechanical properties than other specimens. The density, hardness, flexural strength, and weight percentages of Boron nitride (BN) and Titanium diboride ( $\text{TiB}_2$ ) phases in the specimen with 5 wt% molasses were  $2.36 \text{ g/cm}^3$ , 64 HRA, 31.5 MPa, 68.9%, and 31.1%, respectively. The use of evaporation vessel waste and molasses in the production of crucibles in this study is in line with Sustainable Development Goals (SDGs) 3, 7, 14, and 15, which relate to improving excellent health and well-being, ensuring access to affordable energy, and conserving marine and terrestrial ecosystems.

## 1. Introduction

Plastic metallization is the process of coating plastic components with a thin layer of metal, such as aluminum, in order to give the surface of the plastic a metallic look and make its qualities more comparable to those of metal [1], [2]. Plastic packaging uses aluminum film as an effective barrier against gas, moisture, light, and oxygen to maintain the quality, safety, and aroma of the food products packed inside [3]. There are numerous coating methods for plastic surfaces, including electroplating, thermal spraying, and vacuum coating. Vacuum coating is regarded as one of the most efficient methods for metalizing plastic surfaces [4]. In the vacuum coating process, aluminum is heated in a vacuum chamber until it reaches its melting point, causing its atoms and molecules to vaporize and adhere to the moving plastic surface [1]. Evaporation boats (Fig. 1) are critical components in the process of plastic metallization, enabling controlled evaporation of metals onto plastic surfaces to acquire the appropriate metallic characteristics. However, to guarantee the efficiency of the plastic metallization process, it is necessary to replace the evaporation boats every 15 h [1], [5].

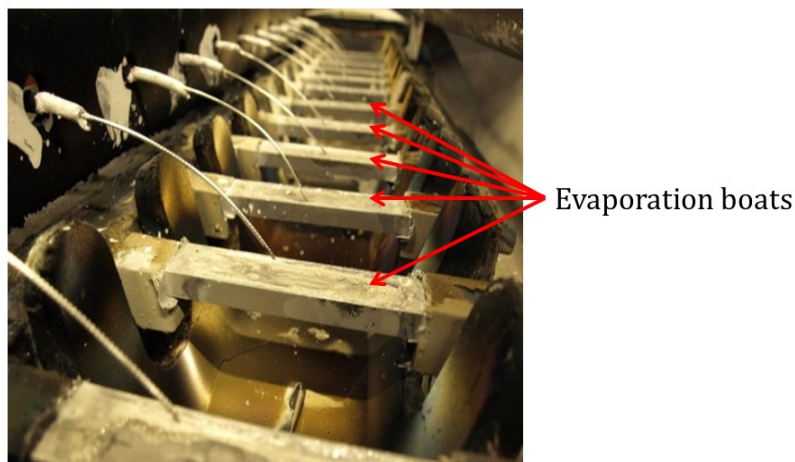


**Fig. 1** Evaporation boats in the plastic metallization process [6]

The evaporation boat waste has a similar composition to virgin evaporation boats made from conductive ceramic materials such as BN and  $\text{TiB}_2$ , which have high mechanical strength, thermal stability, and melting points [7], [8]. Boron nitride (BN) and titanium diboride ( $\text{TiB}_2$ ) have remarkable properties such as outstanding resistance to wear, great hardness, stability at high temperatures, and a high melting point. This makes it easier to use BN and  $\text{TiB}_2$  in many industrial processes, such as metallic evaporation plating, wear-resistant coatings, and aerospace applications [9–11]. Composite ceramics made of  $\text{TiB}_2$  and BN are good at conducting electricity, resist wear well, and are easy to machine [10, 12]. Moreover, the combination of  $\text{TiB}_2$  with BN provides enhanced electrical conductivity and lubricating properties for molten metals [10]. Based on the previous description,  $\text{TiB}_2$ -BN is a suitable material for the manufacture of crucibles due to its superior properties, including chemical stability, corrosion resistance, thermal shock resistance, high-temperature resistance, thermal and electrical conductivity [8], [10].

A crucible is a specialized container designed to withstand high temperatures and is primarily used for heating substances to very high temperatures, often to melt or fuse them. Although clay and graphite are commonly used for crucibles, other materials like ceramics, metals, and quartz can also be used depending on the specific application. Additionally, modern crucibles can be made with advanced, high-temperature resistant materials such as alumina, zirconia, and platinum [13]–[17]. The attractive qualities of crucible materials have attracted the attention of researchers, academics, and businesses worldwide.

From 2020 to 2023, 2315 research paper documents have been published in Scopus-indexed journals with the keyword crucible. The number of research articles in 2020, 2021, 2022, and 2023 is 574, 573, 598, and 570, respectively (Scopus, January 2024, Search: "Crucible"). Large volumes of evaporation boat waste and molasses are generated by the plastic metallization industry and the sugar processing industry, respectively. Improper waste management can negatively affect the environment and human health [18]. Therefore, one possible solution is to recycle with the use of evaporation boat waste and molasses as raw materials for the production of crucibles. This strategy can aid in the reduction of pollution while simultaneously supporting the Sustainable Development Goals (SDGs), specifically goals 3, 7, 14, and 15, which pertain to health and well-being, affordable energy, and the conservation of marine and terrestrial ecosystems [19]. By utilizing evaporation boat waste and molasses as crucible raw materials, multiple benefits are attained simultaneously. Initially, it assists in diminishing the quantity of waste products disposed of in the environment, thus alleviating the adverse impacts on ecosystems and human well-being. Furthermore, stakeholders can create novel items that possess enhanced worth for both the industry and society through the process of recycling this trash. This aligns with SDG Objective 9, which prioritizes the development of industry, innovation, and infrastructure. Thus, the recycle of evaporation boat waste and molasses as raw materials for manufacturing crucibles can be a sustainable solution for reducing industrial waste, protecting the environment, and advancing the SDGs in general [19].

As far as the author's knowledge, the manufacture of crucibles using evaporation boat waste with molasses as a binder is rarely investigated. This is shown by the fact that only three papers have been published in Scopus-indexed journals with the keyword's crucibles and evaporation boat waste (Scopus, January 2024, Search: "crucible" and "evaporation" and "boat" and "waste"). Using evaporation boat waste as a material for making crucibles is one solution to overcome the waste generated by the plastic metallization industry. This is because evaporation boats are made of materials such as BN and TiB<sub>2</sub>, which have very suitable characteristics for making crucibles. Binders are required for the production of crucibles in order to hold the raw materials together during the manufacturing process and provide the necessary strength and durability [20]. Clay, oxidation-resistant materials, hybrid binders, carbon binders, liquid coal tar, and kaolin clays are commonly used as binders for crucible manufacturing, especially graphite crucibles [21]–[25]. Molasses is produced as a byproduct of sugar refining. Due to the unique properties that make it an effective binder, it is frequently used as a binder in a variety of industrial applications [26]–[28]. The utilization of molasses in this study was designated to increase the molecular bonds between particles to produce crucibles with high mechanical properties and reduce the cost of making crucibles. In addition, molasses has been widely used and researched as a binder for manufacturing fly ash mixed concrete, iron pellets, refractory ceramic bricks and biofuel pellets [28]–[31]. The objective of this investigation is to ascertain the physical and mechanical properties of crucibles produced from evaporation boat waste, utilizing different concentrations of molasses as a binder.

## 2. Materials and Methods

The evaporation boat waste used in this investigation was obtained from PT 3M Indonesia. Evaporation boats are composed of BN and TiB<sub>2</sub>. Density, hardness, Young's modulus, flexural strength, and thermal conductivity on evaporation boats were > 2.75 g/cm<sup>3</sup>, 45 HB, 55 GPa, 70 MPa, and 80 W/m.K. (at 20°C), respectively [7]. The molasses used as a binder in this study were purchased from Putra Agro Lestari Store, Salatiga, Indonesia. The characteristics and chemical elements of molasses are shown in Table 1.

**Table 1** The characteristics and chemical elements of molasses [32]–[36]

Test Parameters	Values
Density (g/cm <sup>3</sup> )	1.35–1.44
Total sugar (%)	51–51.36
Ash (%)	7–15
Water (%)	12–47
Sucrose (%)	29–40
Glucose (%)	4–14
Fructose (%)	3–6
Solubility	Water soluble
Dynamic viscosity at 27°C (mPa.s)	3338

Fig. 2 shows a schematic illustration of the process for fabricating crucible specimens. The evaporation boat waste is crushed with a crusher machine and filtered through a 100-mesh sieve to produce evaporation boat waste powder [8]. The evaporation boat waste powder and molasses were mixed using a mixer at 1400 rpm for 30 minutes. In this study, the concentration of molasses used was 0 wt.%, 5 wt.%, 10 wt.%, 15 wt.%, and 20 wt.%. To facilitate the production of a uniform mixture, 60 ml of water is added during the mixing process. The material composition of each specimen is shown in Table 2. The material that has been mixed homogeneously is put into

the mold, and the mixture was compressed at a pressure of 25 MPa to create a green body.

The green body formed is dried in an oven for 300 minutes at 100°C. After drying, the green body is fired at 1150°C with a holding time of 240 minutes.

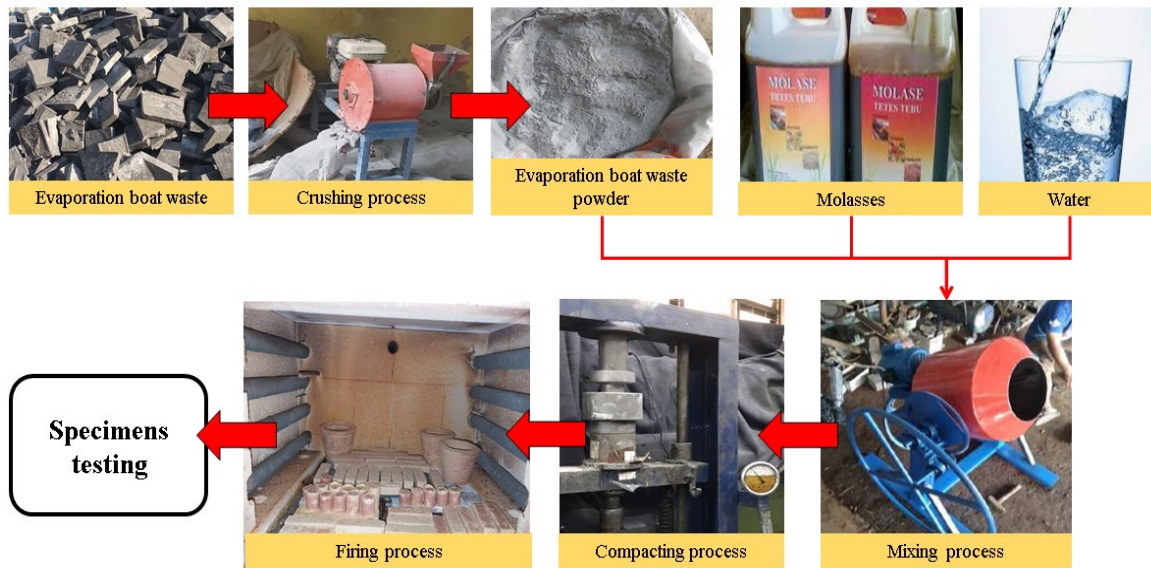


Fig. 2 Schematic illustration of the process for fabricating crucible specimens

The firing process was carried out to increase the hardness and strength of the crucible specimens produced [37]. In the failure of the green body formation during compaction, the specimens containing 15% and 20% Molasses were not subjected to the firing process (Fig. 3). An excessive quantity of moisture is produced by a high molasses concentration, which inhibits the creation of a green body after compaction.

Table 2 Label and composition of crucible specimens

Code of specimens	Evaporation boat waste (powder) (wt.%)	Molasses (wt.%)
0% Molasses	100	0
5% Molasses	95	5
10% Molasses	90	10
15% Molasses	85	15
20% Molasses	80	20

Evaluation of the properties of the obtained specimens was carried out using XRD, SEM, hardness, density, and three-point bending tests. A scanning electron microscope (SEM) (JSM-6510, JEOL, Tokyo, Japan) was used to examine the surface morphology of the specimens at an appropriate accelerating voltage of 15 kV. A high-sensitivity electron detector was affixed to the bottom of the objective lens to generate composition images, topography images, and shadow images [38]. Crystal phase analysis was performed on samples obtained from molasses and evaporation boat waste products using a Shimadzu XRD-7000 (Shimadzu Corporation, Kyoto, Japan). Version 3.0e of High Score Plus was used to perform the Rietveld analysis. The diffraction line profiles on Rietveld smoothing are described by pseudo-Voigt functions [39], [40].

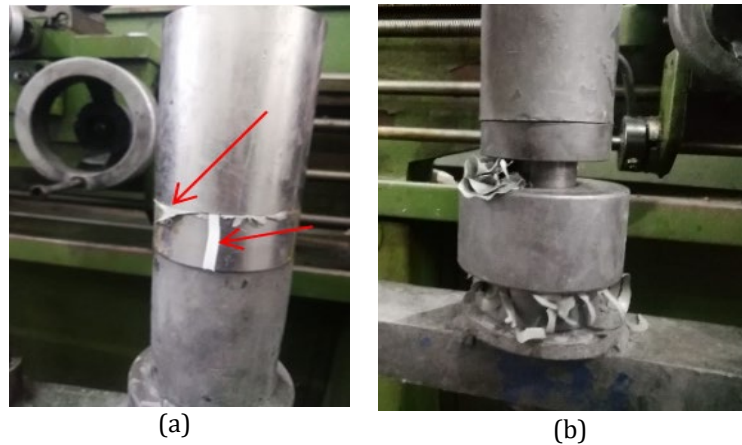


**Fig. 3** Green bodies that failed to form in (a) 15% molasses; and (b) 20% molasses specimens

The specimens obtained from this study conducted a hardness test utilizing the Rockwell hardness type-A method with a force of 60 KgF according to ASTM C748-20. The methodology employed for hardness testing in this investigation is based on the findings of Qi et al. (2019). The researchers employed the Rockwell hardness type-A method to ascertain the hardness of  $TiB_2$ -Fe-Co materials that underwent treatment and heating at a range of temperatures (800°C–1200°C) [41]. By ASTM C1161-18 specifications, the flexural strength and modulus of the specimen were ascertained via the three-point bending test. For the 3-point bending test in this investigation, a Hung Ta Instrument Co., Ltd., Samutprakarn, Thailand HT-2402 Series Computer Universal Testing Machine was utilized. ASTM C20-compliant electronic density meters (DME 220 series) manufactured by Vibra Canada Inc. (Mississauga, Ontario, USA) were utilized to determine the density. Fig. 4 displays the dimensions of the testing specimens used in this study.

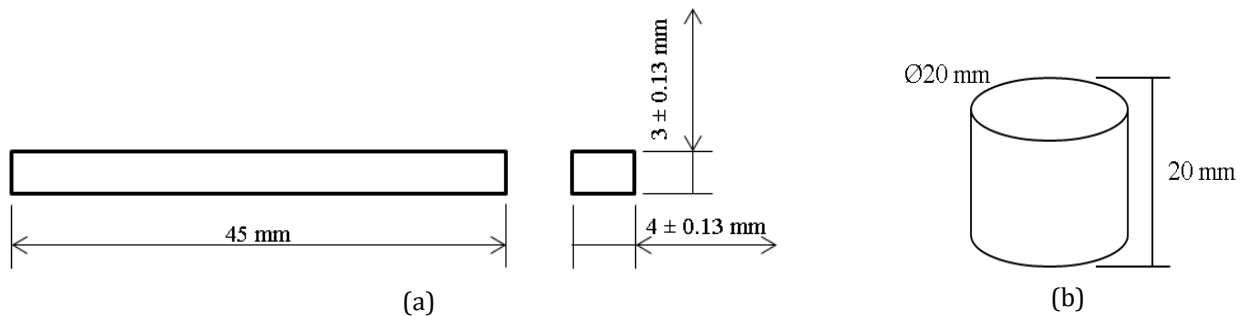


**Fig. 4** Specimen dimensions for (a) three-point bending; and (b) density testing

### 3. Equations Results and Discussion

#### 3.1 Physical Properties Characterizations

The results of the SEM test with a magnification of 2500 times are shown in Fig. 5. The SEM image shows that the crucible specimen consists of large and flaky grains, each showing  $TiB_2$  and BN.

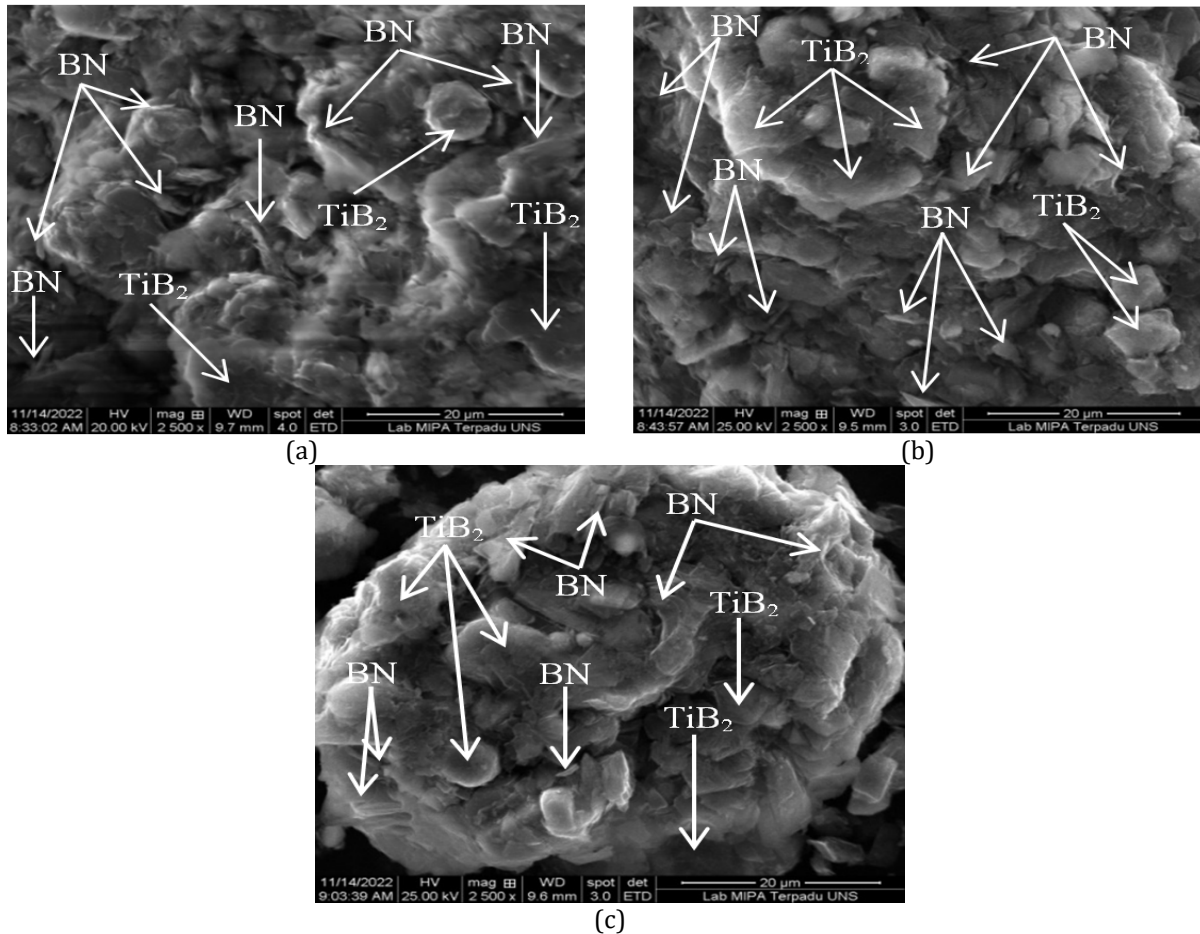


**Fig. 5** SEM images of the crucible specimens (a) 0% molasse; (b) 5% molasses; and (c) 10% molasses

The results of this study are the same as those performed by Tian et al. (2022) and Popov et al. (2022), which stated that large and flaky grains each show the presence of  $\text{TiB}_2$  and BN [10], [42]. According to research conducted by Tian et al. (2022), the volume ratio of  $\text{TiB}_2$ -SiC influences the SEM image of the resulting  $\text{TiB}_2$ -BN-SiC composite ceramic significantly. The SEM test revealed that the morphology of the composite ceramic  $\text{TiB}_2$ -BN-SiC consisted of large crystal grains and numerous flake crystals. The lamellar crystal structure is the BN phase, and the  $\text{TiB}_2$  phase and SiC phase grains are dispersed among the BN crystal. As the proportion of  $\text{TiB}_2$  to SiC rises there is a significant increase in the size of  $\text{TiB}_2$  crystals. This phenomenon arises due to the augmentation of the  $\text{TiB}_2$  phase's relative content, resulting in enhanced inter-particle interaction within the  $\text{TiB}_2$  phase. Consequently, bonds within  $\text{TiB}_2$  particles consolidate, leading to the formation of larger grains [10]. The scanning electron microscopy (SEM) photos discovered by Popov et al. (2022) illustrate the fracture surfaces of  $\text{TiB}_2$ -BN-C materials. These materials were produced by hot-pressing TiN-B<sub>4</sub>C particle precursors at different temperatures. The photos depict the generation of platelet-shaped inclusions, specifically characterized as boron nitride, and also non-platelet-shaped graphite inclusions. The EDS mapping analysis of the shattered  $\text{TiB}_2$ -BN-C surface provides evidence of the existence of plate-like inclusions composed of boron nitride. Furthermore, the scanning electron microscopy (SEM) study of backscattered electrons indicates that the plate-like grains consist of lighter materials, specifically likely h-BN or graphite [42]. The findings of this investigation suggest that including molasses in the production of crucibles does not have a substantial impact on the resultant SEM image. This outcome diverges from the findings of the studies done by Tian et al. (2022) and Popov et al. (2022). The researchers discovered variations in the SEM pictures as a result of various settings in volume fraction [10] and hot-pressing temperatures [42] employed during the preparation of the specimens.

The XRD test findings (Fig. 6) for each specimen indicated that the presence of molasses and the preparation of the specimens didn't result in the creation of a new phase. The specimens exhibited exclusively  $\text{TiB}_2$  and BN crystals, without any other peaks detected. The  $\text{TiB}_2$  crystal phase displays distinct intensity peaks at specific angles, referred to as  $2\theta$ , which have been determined at 26.7, 34.2, 44.4, 57.0, 61.1, 68.1, 71.4, and 78.6. These values correspond to the JCPDS card No. 35-0741. The intensity peak observations of the  $\text{TiB}_2$  crystal phase acquired in this investigation exhibit a similar trend to those reported in previous studies conducted by Nguyen

et al. (2020), Ahmadi et al. (2019), and Shayesteh et al. (2019) [43]–[45]. The study found that the BN crystal phase displayed distinct intensity peaks at specific angles, specifically  $2\theta$ : 26.7, 41.6, 44.5, 48.7, 53.8, and 74.8. These peaks correspond to the JCPDS card No. 85-1068. The intensity peak findings of the BN crystal phase obtained have the same trend as the intensity peak findings in studies conducted by Shaddel, et al., (2020) and Vafa, et al., (2020) [46], [47].

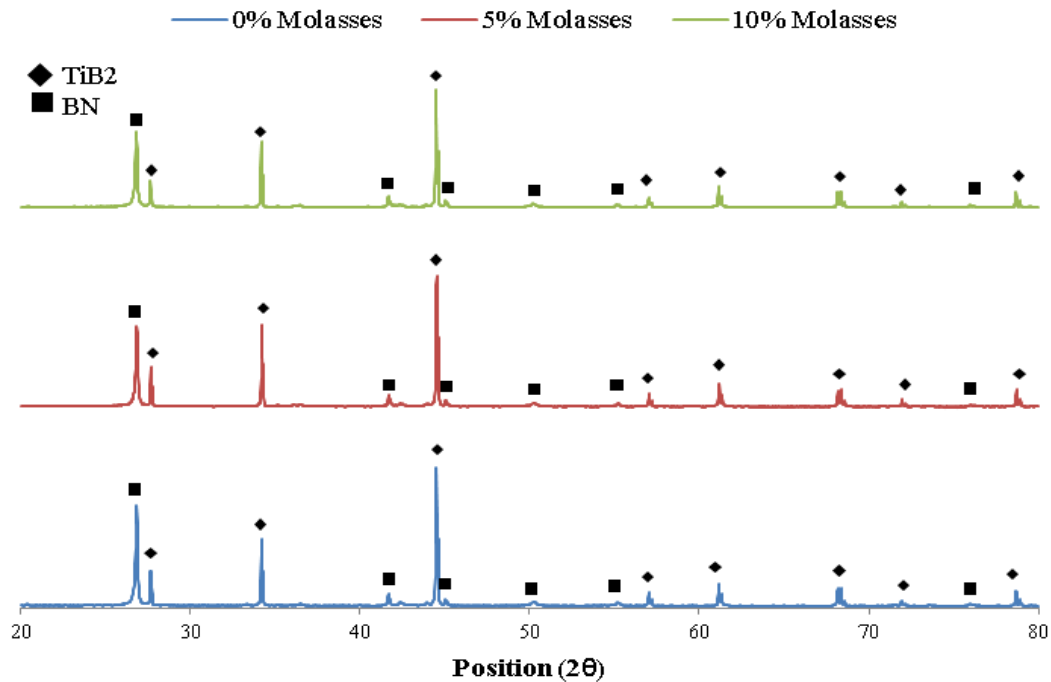


**Fig. 6** XRD pattern of the crucible specimens with various concentrations of molasses

The XRD test results obtained in this study showed that the use of molasses in the crucible specimens did not form a new crystalline phase after the firing process. Molasses is an organic compound with sucrose, glucose and fructose content of 32%, 14% and 16% [15]. Molasses typically consists of elements of Carbon, Hydrogen, Oxygen, Nitrogen, and Sulphur [48].

Based on research conducted by Zhai, et al., (2018), by conducting ultimate analysis tests on molasses, it states that the most elemental content possessed by molasses is C atoms (Carbon) with a percentage of 47.40%. In their XRD test results, the unreadable peak intensity of the Carbon crystal phase is the result of the firing process treatment [48]. Hamzah et al. (2023) investigated the impact of fire temperature on silica nanoparticles synthesized with 1% molasses. Due to the addition of molasses, the EDS test revealed that the sample contained only a small percentage of carbon (5.9 wt%). However, the firing procedure evaporates most of the molasses, leaving only a trace amount in the sample. This is the reason why XRD diffraction is unable to identify the peaks on the carbon crystals [49].

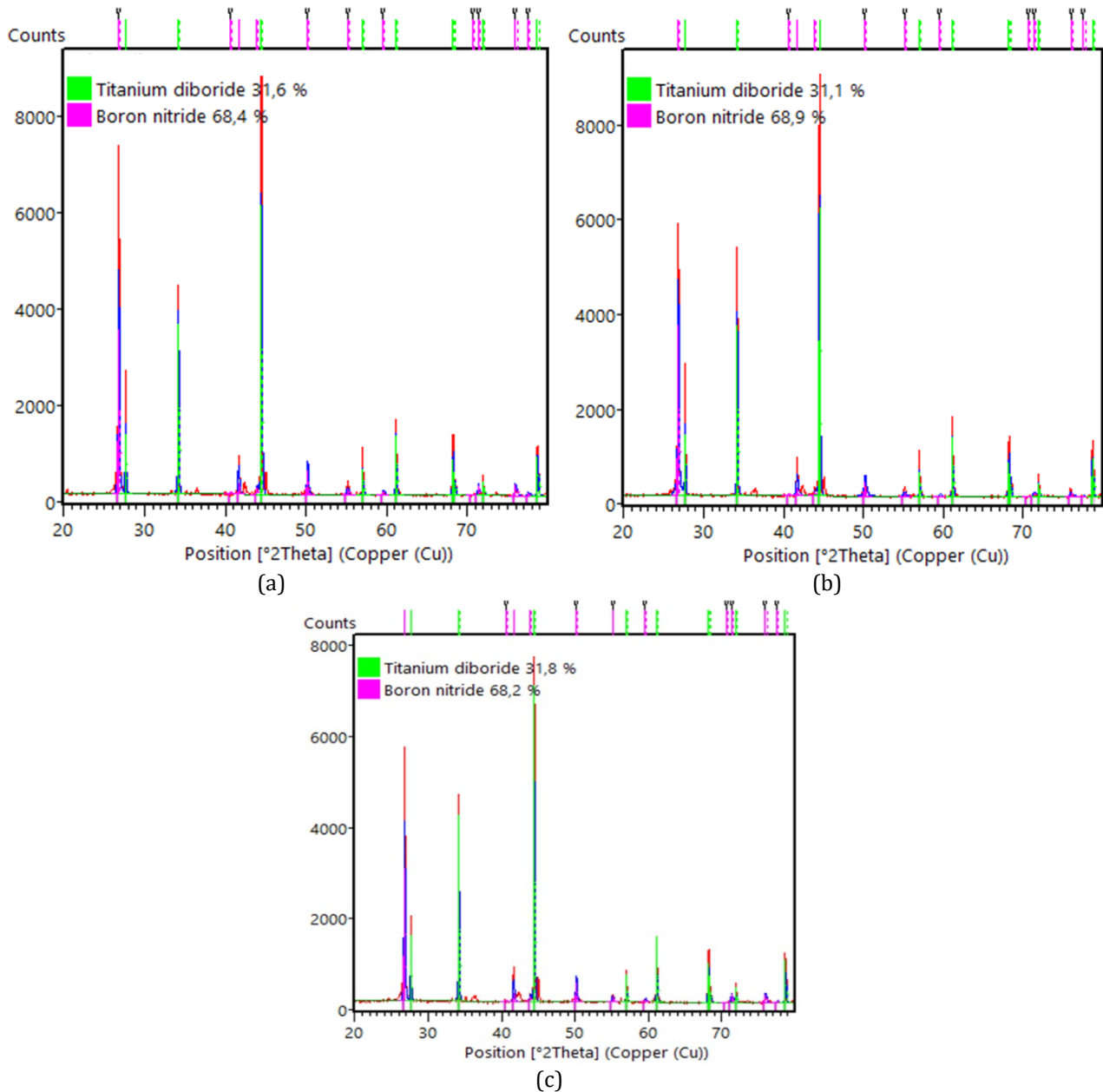


**Fig. 7** Rietveld analysis using high score plus software on the (a) 0% molasse; (b) 5% molasses; and (c) 10% molasses specimens

The XRD test results can be used to determine the weight percentage (%) of the TiB<sub>2</sub> and BN crystal phases for each specimen formed. Weight percentage was analyzed using High Score Plus software with the Rietveld Analysis method (Fig. 7). The analysis showed that samples with a molasses concentration of 0% produced a weight percentage of the BN phase of 68.4% and a weight percentage of the TiB<sub>2</sub> phase of 31.6%. Using molasses with a concentration of 5% resulted in a weight percentage of the BN phase of 68.9% and a weight percentage of the TiB<sub>2</sub> phase of 31.1%. Whereas in specimens with a molasses concentration of 10%, the weight percentages of BN and TiB<sub>2</sub> phases were 68.2% and 31.8%. Fig. 8 shows that adding molasses concentration from 0% to 5% can increase the weight percentage of the BN phase and decrease the weight percentage of the TiB<sub>2</sub> phase. However, when the concentration of molasses was added from 5% to 10%, the weight percentage of the BN phase decreased and increased the weight percentage of the TiB<sub>2</sub> phase.

In this study, the change in weight percentage within the BN and TiB<sub>2</sub> phases was caused by the firing treatment during specimen formation [45]. The growth of the TiB<sub>2</sub> phase can be observed at a firing temperature of 1150°C and will increase when given a higher firing temperature [50]. However, a study conducted by Tong, et al., (2008) showed that the presence of the BN phase could inhibit the growth of other compound phases [51]. Research conducted by Popov et al. (2022) shows the formation of TiB<sub>2</sub> crystals on TiN-B<sub>4</sub>C at hot pressing at 1100°C. The intensity of the TiB<sub>2</sub> crystal peaks was getting stronger with increasing the pressing temperature,

which was carried out at 1100°C–1900°C. Nevertheless, when the temperature reached 1900°C, the intensity of the TiB<sub>2</sub> crystal peak reduced as a result of the increased intensity of the h-BN crystal peak [42]. Therefore, an increase in the amount of BN phases will result in a reduction of the TiB<sub>2</sub> phase in crucible specimens when using molasses with concentrations of 0%, 5%, and 10%. The XRD analysis performed by Dey et al. (2022) likewise exhibited an identical pattern. The findings of their study demonstrated a correlation between a rise in the BN phase and a subsequent decrease in the TiB<sub>2</sub> phase. Their research revealed that the inclusion of h-BN particles in the Ti-rich layer's matrix contributed to a reduction in the resulting coefficient of friction. The Al<sub>2</sub>O<sub>3</sub>-TiB<sub>2</sub>-TiN-BN composite ceramic coating is suitable for tribomechanical applications on the Ti-6Al-4V alloy [52].

According to the findings of this study, the weight percentage of the BN phase is consistently higher compared to the weight percentage of the TiB<sub>2</sub> phase in all of the crucible specimens that were fabricated. The results of this study align with the research carried out by Habiby et al. (2022). According to their research, the evaporation boat waste contains a high concentration of Boron (B) and Nitrogen (N), accounting for 43.68% and 34.98% respectively. The evaporation boat waste exhibits the main constituents of Boron and Nitrogen [5]. The results of this investigation align with the research carried out by Tian et al. (2022). The X-ray diffraction (XRD) analysis of their research revealed that the presence of TiB<sub>2</sub> and BN peak diffraction patterns was observable in all of the tested samples. As the sintering temperatures rise, the peak indicating the presence of the BN phase becomes gradually narrower. It illustrates that as the temperature increases, the crystallization capability of the BN phase improves, resulting in a purer BN matrix. The investigation has revealed several impurity peaks, such as FeO, Fe<sub>3</sub>Si, as well as FeB [10].

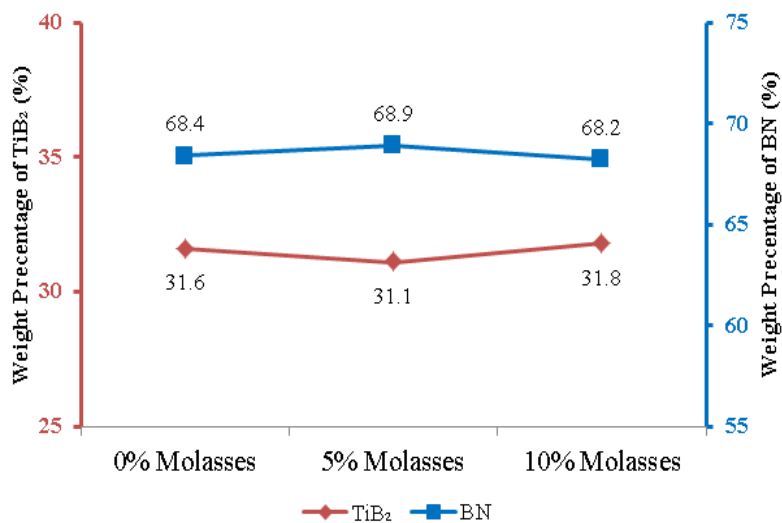


**Fig. 8** Comparison of weight percentage phase of BN and TiB<sub>2</sub> of the crucible specimens

### 3.2 Mechanicals Properties Characterizations

This study indicates that the concentration of molasses significantly affects the density of crucible specimens (Fig. 9). Specimens with a 0% molasses concentration had the lowest density (2.07 g/cm<sup>3</sup>). Specimens with 5% and 10% molasses concentrations had densities of 2.36 g/cm<sup>3</sup> and 2.20 g/cm<sup>3</sup>, respectively. According to the findings of this study, the presence of molasses at a concentration of 5% can result in a higher density than other specimens. The objective of adding molasses as a binder in the present study was to effectively consolidate BN-TiB<sub>2</sub> particles. Molasses aid in enhancing the structural integrity of BN-TiB<sub>2</sub> particles by promoting cohesion and stability. Crucibles manufactured using binders exhibit a greater density and enhanced durability in comparison to specimens lacking molasses [53]. Molasses, derived from the sugar manufacturing process, contain a significant amount of moisture. Molasses can increase the product's water content when used as a binder or additive [54]–[56]. This increase in water content can result in a reduction in density due to the displacement of other materials and the occupation of space in the container by the water [54], [57].

The research findings align with the study performed by Utchariyajit, et al., (2019). Their research employed molasses as a binding agent for briquettes manufactured from palmyra trash to assess their physical characteristics and calorific value. The molasses concentration employed was 5%, 10%, and 20%. The research findings indicated that a 5% concentration of molasses exhibited the highest density value, whereas an increase in molasses concentration led to a fall in density value [54]. The bulk density of the briquette samples exhibited an upward trend with a 6% binder concentration in the mixture, as reported by Deshannavar et al. (2018) [58]. However, increasing the binder concentration further led to a decline in the bulk density values. Syahfitri et al.

(2022) established a direct correlation between the rise in molasses content and the decrease in density of the composite lightweight roof tile. Using a 10% concentration of molasses achieves a roof tile combination with the maximum density [59]. Jiménez et al. (2022) also obtained similar results in their study. With a 2% molasses concentration, a composite with a high density is produced. As molasses concentration rises, the composite's density reduces [60].

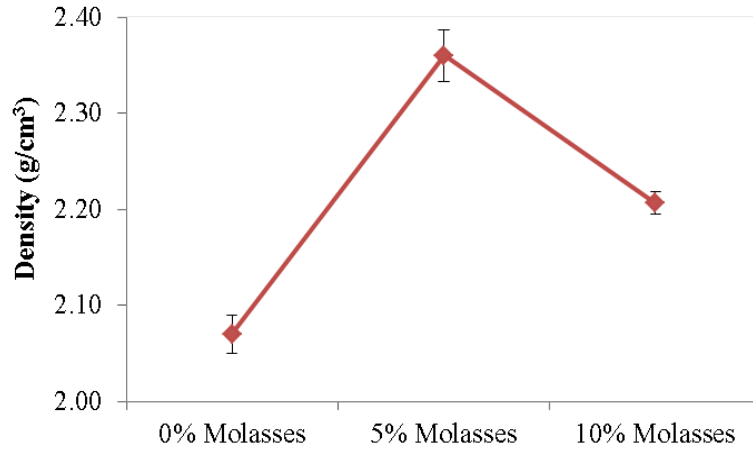


**Fig. 9** The density of the crucible specimens with various concentrations of molasses

According to the findings of this study, the use of 5% molasses produced the highest crucible density. This occurs because at this concentration, the molasses and evaporation boat waste powder mixture become more homogenous, resulting in stronger bonding and fewer pores. Furthermore, the higher the molasses concentration employed, the higher the water content in the mixed material. Higher water content promotes coalescence, which aids particle adherence and granule growth. However, as a result of the water evaporation, the water content will decrease during the firing process, causing pore formation. Higher moisture content causes increased pore formation, increased porosity, and decreased density [61]–[63]. Liu et al. (2022) [64] found that the density of Cf/C–SiC composites increases consistently as the binary binder content increases. The study conducted by Yu et al. (2010) revealed that the porosity of porous silicon nitride ceramics is affected by the ratio of binders used. Increasing the concentration of binder leads to a higher level of porosity. The majority of the pores in the sintered body originate from the residual micro-spaces left by the organic processing aids after the organic binder has been burned off in the green body [65]. In addition, a study performed by Ayorinde et al. (2013) demonstrated that there was a reduction in the density of particles as the concentration of molasses increased [66].

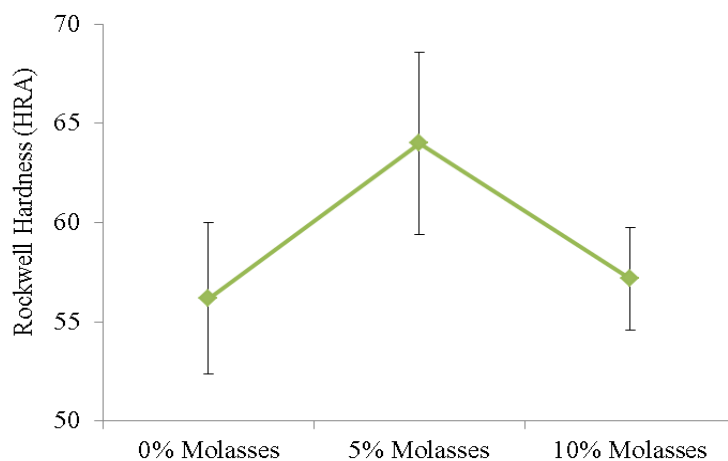


**Fig. 10** The effect of molasses concentration on the hardness produced in crucible specimens

Fig. 10 shows the effect of molasses concentration on the hardness of crucible specimens. Hardness increased in the specimens with increasing molasses concentration from 0% to 5%. However, the hardness of the crucible specimens decreases when using molasses with a concentration exceeding 5%. Using molasses with a concentration of 5% is the best composition compared to the other specimens. From the research results it can

also be seen that specimens with the addition of molasses produce crucibles with higher hardness than specimens without the addition of molasses. The highest hardness of 64 HRA was found in specimens using molasses with a concentration of 5%. The lowest hardness was found in specimens with 0% molasses concentration, which was 56.17 HRA. Meanwhile, specimens with 10% molasses concentration produced a hardness of 57.17 HRA.

The results showed that hardness is directly proportional to density in crucible specimens (Fig. 11). A material's hardness is proportional to its density. According to the findings of this study, increasing the concentration of molasses from 0% to 5% increases both the density and the hardness of the crucible specimens. In contrast, a decrease in the specimen's density when using a molasses concentration greater than 5% is accompanied by a reduction in its hardness. In this study, hardness increased with increasing density. This correlation makes it reasonable because closer packing of atoms results in higher density and shorter bond lengths, which results in higher hardness.

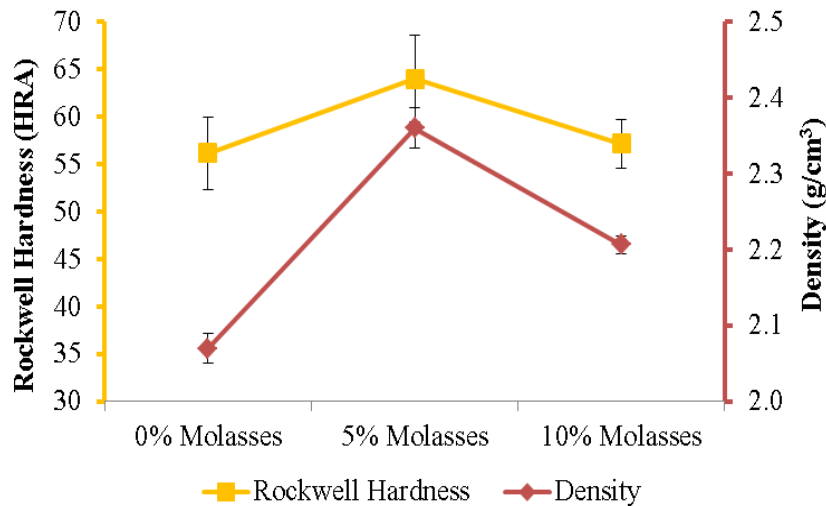


**Fig. 11** Relationship between density and rockwell hardness on crucible specimens

The relationship between density and hardness values is also found in research conducted by Babapoor, et al., (2018). According to their study, raising the spark plasma sintering (SPS) temperatures from 1800°C to 1900°C resulted in an increase in density, which was then followed by an increase in Vickers hardness. At temperatures ranging from 1900°C to 2000°C, the SPS treatment can effectively lower the density, resulting in a subsequent fall in Vickers hardness [67]. As the amount of porosity decreases, the density of crucible samples increases [68]. The density of the 5% Molasses specimen is higher than that of the other specimens. This demonstrates that specimens containing 5% molasses have lower porosity than other specimens. A material's porosity content affects its hardness, with less porosity resulting in higher hardness [69]. This explains why the 5% molasses specimen is harder than the others. As porosity increases, the structural integrity of the material degrades because void space disturbs the material's structural continuity. The presence of pores creates material defects or weak points that can function as stress concentrators. When forces are applied to the material, these weak points are more susceptible to deformation than the denser regions. Consequently, the material becomes less resistant to indentation and abrasion, resulting in a reduction in hardness [69].

The flexural test results show that the flexural strength and flexural modulus values on the crucible specimens have a linear relationship (Fig. 12). The addition of molasses concentration from 0% to 5% was able to increase the flexural strength and flexural modulus. However, when molasses concentration was added from 5% to 10%, the flexural strength and flexural modulus decreased. The flexural test results showed that adding 5% molasses concentration produced the highest flexural strength and flexural modulus. Flexural strength in crucibles with molasses concentrations of 0%, 5%, and 10% were 29.82 MPa, 31.5 MPa and 21.1 MPa. The flexural modulus of crucibles containing molasses concentrations of 0%, 5%, and 10% were 15.59 GPa, 17.5 GPa, and 13.39 GPa, respectively. The study conducted by Singh et al. (2018) showed a relationship between flexural modulus and flexural strength results. Their research focused on the inclusion of SiO<sub>2</sub> to improve the tensile and flexural properties of SiO<sub>2</sub>-Epoxy nanocomposite polymers. The findings from their study showed that the addition of SiO<sub>2</sub> at different weight percentages (0 wt.%, 2 wt.%, and 4 wt.%) increased the flexural strength and flexural modulus of the samples. On the other hand, an increase in SiO<sub>2</sub> content beyond 4% resulted in a decrease in flexural strength, which was accompanied by a decrease in flexural modulus [70].

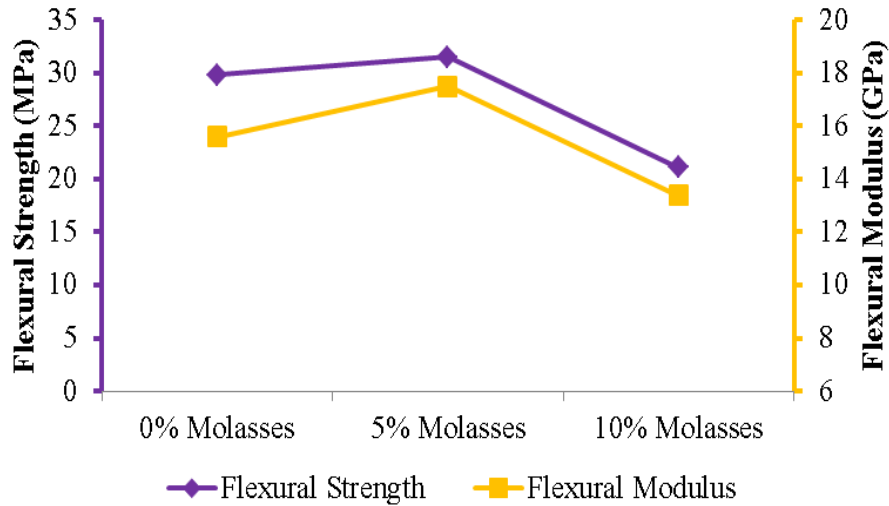


**Fig. 12** Flexural properties of the crucible specimens with various concentrations of molasses

Flexural testing is a method used to assess the mechanical characteristics of a material. The mechanical characteristics of the material are affected by its physical qualities, including the density value (Fig. 13). Increasing the density value directly correlates with an increase in the mechanical properties of the material [38], [71], [72]. These findings align with the results of the study, which observed that the flexural strength increased as the density increased from 0% to 5% molasses content. Specimens utilising molasses at concentrations ranging from 5% to 10% saw a reduction in density, which subsequently led to a drop in flexural strength. Nevertheless, the investigation's results indicated that the density of the specimen at 0% molasses concentration was lower compared to the density at 10% molasses concentration. Conversely, the flexural strength obtained was higher.

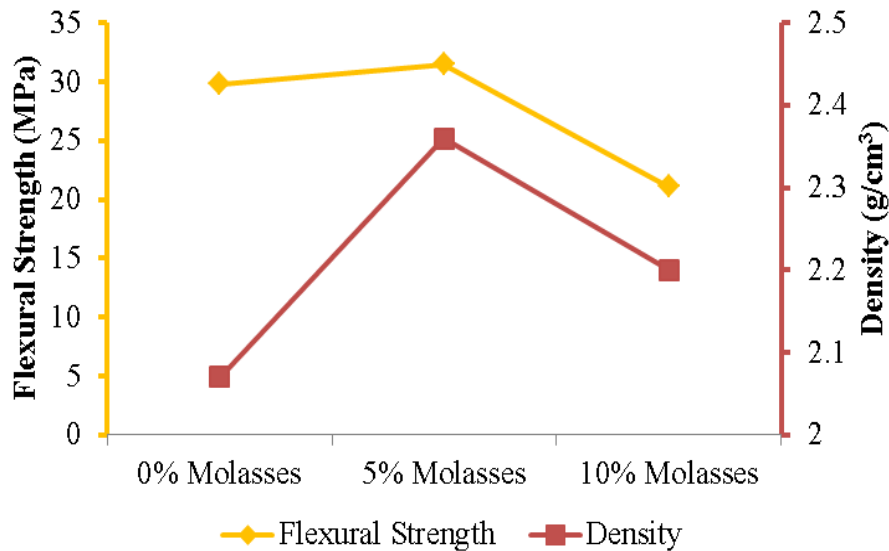


**Fig. 13** Relationship between flexural strength and density on crucible specimens

The flexural strength of the composite specimen is directly related to its material density [73], [74]. The study findings indicated that crucible specimens utilizing molasses with a 5% concentration exhibited superior flexural strength compared to the other specimens. This occurs because this particular specimen possesses the greatest density in comparison to the other specimens. The high density of the material implies a larger mass for each unit of volume. The higher density typically equates to a greater number of atoms or molecules within the substance, leading to greater interatomic or intermolecular connections. Materials possessing greater internal bonding exhibit higher levels of cohesion and structural resilience. It enhances the material's ability to withstand bending forces by increasing its resistance to deformation and fracture. The presence of robust interatomic or intermolecular forces enhances the material's ability to resist and evenly distribute external loads. Furthermore, a substance with a higher density generally exhibits a more compact and homogeneous arrangement. This

decreases the number of voids, pores, and other defects that can function as stress concentrators. The absence of such imperfections decreases the possibility of fracture initiation and propagation, thereby enhancing flexural strength [73], [74].

The discrepancy between density and mechanical properties also occurs in research conducted by Carnaje, et al., (2018) [56] regarding manufacturing charcoal briquettes with molasses binder. In their study, molasses-charcoal was used with variations of 60:40, 70:30 and 80:20. The results showed that the lowest bulk density value was found in the 70:30 variations. However, the 70:30 variations had the highest compressive strength value. This is possible because increasing amounts of molasses can strengthen the bonds between particles, resulting in a higher density. However, increasing the amount of molasses given causes the humidity level to be higher, which causes the material to become softer [56], [75]. This result was also the case for specimens containing 10% molasses, which resulted in lower flexural strength than specimens containing 0% molasses. Even though specimens containing 10% molasses produced a higher density than specimens containing 0% molasses.

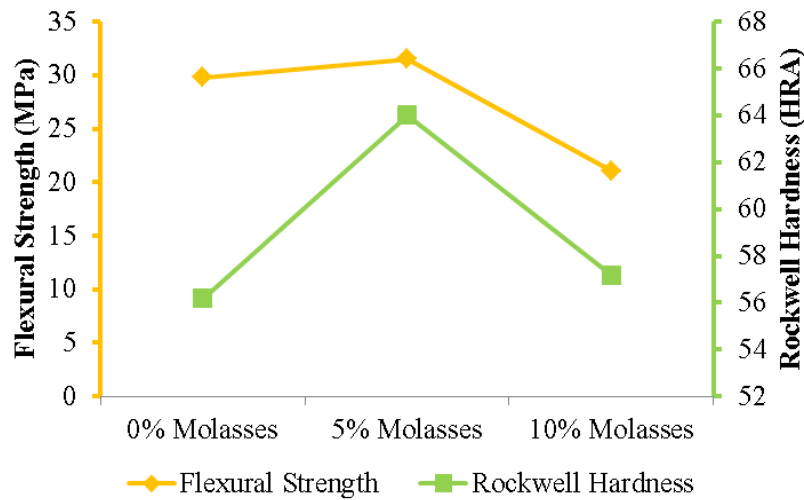


**Fig. 14** Relationship between flexural strength and rockwell hardness on crucible specimens

The highest hardness and flexural strength were obtained from specimens with a concentration of 5% as shown in Fig. 14. However, at a concentration of 0%, they had a lower hardness and a higher flexural strength than specimens using molasses with a concentration of 10%. Differences in hardness and flexural strength test results also occurred in a study conducted by Changchun et al., (2020) regarding the effect of adding ZrC to WC–Ni hard metals using the spark plasma sintering method. The results demonstrated that increasing the ZrC content from 0% to 3% enhanced the Vickers hardness. However, the Vickers hardness decreased as the ZrC concentration exceeded 3%. In the flexural strength results, the addition of ZrC decreased the value of flexural strength. This is due to several reasons, including the formation of ZrO<sub>2</sub>, the reduced strength of the metal bonding phase, and the agglomeration of the nano-powder [76]. These studies have similarities with the results of this study which have different test results but the values are in a certain range and have the same trend on the graph.

The decrease in flexural strength value in crucible specimens with a molasses concentration of 10% is inseparable from the growth of the BN crystal phase obtained. In a study conducted by Liu, et al., (2021) stated that an increase in BN can increase the flexural strength of the material [77]. The specimen with a molasses concentration of 10% produced the lowest weight percentage of the BN crystal phase, which was 68.2%. This value is lower than the specimen's using molasses with 0% and 5% concentrations. This is why the specimen with a molasses concentration of 10% has the lowest flexural strength. In this study, the molasses addition at 5% concentration Molasses specimens produced the higher physical and mechanical properties compared to other specimens. In the 5% Molasses specimen, density, hardness, flexural strength and flexural modulus values were 2.36 g/cm<sup>3</sup>, 64 HRA, 31.5 MPa, and 17.5 GPa.

**Table 3** Comparison of properties with previous studies

Crucible Raw Materials	Density	Hardness	Flexural strength	Reference
BN	2.1 g/cm <sup>3</sup>	56.5 HRA	20.68 MPa	[78]
Graphite	1.74 g/cm <sup>3</sup>	73.6 HRA	22.1 MPa	[79], [80]
ZrO <sub>2</sub>	6.01 g/cm <sup>3</sup>	85.1 HRA	900 MPa	[81]
Stainless steel	7.78 g/cm <sup>3</sup>	67.9 HRA	-	[82]

Crucible Raw Materials	Density	Hardness	Flexural strength	Reference
Alumina oxide	3.9 g/cm <sup>3</sup>	86 HRA	414 MPa	[83]
Evaporation boat waste	2.36 g/cm <sup>3</sup>	64 HRA	31.5 MPa	5% Molasses specimen (current study)

The density of the 5% Molasses specimen is greater than the density of commercial crucibles made from BN and graphite. Table 3 compares the properties obtained in this study with commercial crucible products or crucibles produced in previous studies. In general, the crucibles produced in this study produced lower densities than ZrO<sub>2</sub> crucibles, Stainless steel crucibles, and Alumina crucibles. The 5% Molasses specimen has higher density and flexural strength than the BN and graphite crucible. Meanwhile, the hardness of the 5% Molasses specimen was higher than that of the BN crucible. However, the hardness of the 5% Molasses specimen was lower than that of the graphite crucible. The research on crucibles made from evaporation boat waste with varying concentrations of molasses is significant in terms of waste utilization, resource efficiency, reduction of environmental impact, and prospective practical applications.

The results of this study may assist in the advancement of sustainable manufacturing techniques, economically efficient production processes, and the exploration of substitute materials for crucible fabrication. Furthermore, the findings align with several Sustainable Development Goals (SDGs). It supports the goal of SDG 7, which aims to provide affordable and sustainable energy, by advocating for the utilization of waste materials and other sources of energy. In addition, the research indirectly supports the improvement of human well-being and the environment by reducing the negative impacts of pollution, in line with Sustainable Development Goal 3. Furthermore, through the practice of reusing waste and minimizing contamination, the study aligns with Sustainable Development Goals 14 and 15, which aim to safeguard terrestrial and marine ecosystems. The investigation on crucibles fabricated from discarded evaporation boats with different levels of molasses showcases a dedication to sustainable methodologies, optimal utilization of resources, and responsible management of the environment, rendering it pertinent to many Sustainable Development Goals (SDGs). It can bring about beneficial transformation by tackling environmental concerns, promoting sustainable production, and supporting the establishment of a circular economy.

#### 4. Conclusions

This study investigated the potential utilization of evaporation boat waste as raw material for crucible production, using molasses as a binder. Crucibles were successfully produced at molasses concentrations of 0%, 5%, and 10%. However, crucible specimens were not formed with the use of molasses at 15% and 20%. The crucible specimens contained only TiB<sub>2</sub> and BN crystals, as revealed by XRD diffraction. The results of this study indicate that the addition of molasses and the specimen preparation process carried out caused the formation of no new crystal phases. The SEM test results corroborated the XRD analysis, revealing the presence of only BN (flake grains) and TiB<sub>2</sub> (large grains) crystals in the morphology of the crucible specimen. The results of this study show that the addition of molasses has a significant effect on the physical and mechanical properties of the crucible. The best molasses concentration was found in the 5% molasses specimen, as it produced crucibles with higher density, hardness, flexural strength, and modulus than the other specimens. The density of the specimens with molasses concentrations of 0%, 5%, and 10% were 2.07 g/cm<sup>3</sup>, 2.36 g/cm<sup>3</sup>, and 2.20 g/cm<sup>3</sup>. When the concentration of molasses exceeds 5%, the moisture content in the crucible specimen increases, causing more pores to form and the density decreases. The study found that hardness, flexural strength, and flexural modulus all exhibited a positive correlation with density, indicating that when density increased, these properties also increased. The hardness, flexural strength, and flexural modulus of the crucible specimen with a 5% molasses content were 64 HRA, 31.5 MPa, and 17.5 GPa, respectively.

This research supports the Sustainable Development Goals (SDGs) by increasing resource utilization, responsibility for the environment, and access to sustainable energy through the utilization of evaporation boat waste and molasses in the fabrication of crucibles. It is following Sustainable Development Goals (SDGs) 3, 7, 14, and 15, which specifically target pollution, wellness, energy affordability, and the preservation of terrestrial and marine ecosystems.

#### Acknowledgement

This research is supported by Universitas Negeri Semarang (UNNES) through Penelitian Terapan Kelembagaan DIPA PNBP UNNES 2022

#### Conflict of Interest

Authors declare that there is no conflict of interests regarding the publication of the paper.

## Author Contribution

The authors confirm contribution to the paper as follows: **study conception and design:** Rusiyanto Rusiyanto, Rahmat Doni Widodo, Athanasius Priharyoto Bayuseno; **data collection:** Ares Yudi Prasetyo, Deni Fajar Fitriyana, Aldias Bahatmaka, Sudiyono Sudiyono; **analysis and interpretation of results:** Rizki Setiadi, Wara Dyah Pita Rengga, Rifky Ismail; **supervision and formal analysis:** Chusni Ansori, Agustinus Purna Irawan; **writing—review and editing:** Tezara Cionita, Januar Parlaungan Siregar; **draft manuscript preparation:** Anjar Priyatmojo, Wahyu Ramdhani, Ferry arifiadi. All authors reviewed the results and approved the final version of the manuscript.

## References

- [1] Bayus, J. A. (2015) Environmental Life Cycle Comparison of Aluminum-based High Barrier Flexible Packaging Laminates. [Master Thesis, Rochester Institute of Technology], New York, United States.
- [2] Drobny, J. G. (2014). 4-Processing Methods Applicable to Thermoplastic Elastomers. In Handbook of Thermoplastic Elastomers (Second Edition), Plastics Design Library (pp. 33–173). William Andrew Publishing. <https://doi.org/10.1016/B978-0-323-22136-8.00004-1>
- [3] Struller, C. F., Kelly, P. J., & Copeland, N. J. (2014) Aluminum oxide barrier coatings on polymer films for food packaging applications, *Surface and Coatings Technology*, 241, 130–137, <https://doi.org/10.1016/j.surfcoat.2013.08.011>
- [4] Bi, J., Li, L., Peng, J., & Shi, P. (2021) Application of vacuum coating process in metallization of plastic surface, *Journal of Physics: Conference Series*, 2044(1), 1–8. <https://doi.org/10.1088/1742-6596/2044/1/012072>
- [5] Habiby, M. N. A., Rusiyanto, Widodo, R. D., & Sumbodo, W. (2022) Effect of Green Body Heating Rate on Mechanical and Physical Properties of Crucible Materials Made from Evaporation Boats Waste, *REM Jurnal*, 7(1), 19–26. <https://doi.org/10.21070/r.e.m.v7i1.1639>
- [6] Supervac Industries LLP. (2023, June 10). Evaporation Boats. <https://www.supervacoils.com/evaporation-boats/>
- [7] 3M Advanced Materials Division. (2015). 3M™ Evaporation Boats (SDS 10915920) [Data set]. <https://multimedia.3m.com/mws/media/10915920/3m-evaporation-boats-product-information-sheet.pdf>
- [8] Rusiyanto, Irfan, M., Widodo, R. D., Sunyoto, & Fitriyana, D. F. (2023) Effect of drying time on compressive strength, impact strength and macro structure of crucible materials made from evaporation boats waste, graphite and kaolin. *AIP Conference Proceedings*, 2609(1), 1–8. <https://doi.org/10.1063/5.0124101>
- [9] He, Q., Tian, T., Tian, S., Guo, W., Shi, Y., Wang, A., Wang, H., Wang, W., & Fu, Z. (2021) Microstructure and mechanical properties of Tin-TiB<sub>2</sub>-HBN composites fabricated by reactive hot pressing using TiN-B mixture, *Materials*, 14(23), 1–14. <https://doi.org/10.3390/ma14237198>
- [10] Shi Tian, Zelin Liao, Wenchao Guo, Qianglong He, H. W. and W. W. (2022) Effects of theTiB<sub>2</sub>-SiC Volume Ratio and Spark Plasma Sintering Temperature on the Properties and Microstructure of TiB<sub>2</sub>-BN-SiC Composite Ceramics, *Crystals*, 12(29), 1–13. <https://doi.org/10.3390/cryst12010029>
- [11] Song, B., Yang, W., Liu, X., Chen, H., & Akhlaghi, M. (2021) Microstructural characterization of TiB<sub>2</sub>-SiC-BN ceramics prepared by hot pressing, *Ceramics International*, 47(20), 29174–29182. <https://doi.org/10.1016/j.ceramint.2021.07.080>
- [12] Songül, E. E., & Duman, I. (2020). Modeling of TiB<sub>2</sub>-BN Composites as Cathode Materials for Aluminum Electrolysis Cell. In Green Energy and Technology (pp. 817–841). [https://doi.org/10.1007/978-3-030-20637-6\\_40](https://doi.org/10.1007/978-3-030-20637-6_40)
- [13] Hendronursito, Y., Isnugroho, K., & Birawidha, D. C. (2019) Analysis of crucible performance for aluminum scrap casting at small and medium enterprises (SMEs) foundry, *IOP Conference Series: Materials Science and Engineering*, 478(1), 1–7. <https://doi.org/10.1088/1757-899X/478/1/012005>
- [14] Perez-Rangel, N., Flórez-Solano, N., & Espinel-Blanco, E. (2020) Development of the manufacturing technique of crucibles to melt aluminum and improve its physical and mechanical properties by microwave oven. *Journal of Physics: Conference Series*, 1708(12015), 1–7. <https://doi.org/10.1088/1742-6596/1708/1/012015>
- [15] Mahaviradhan, N., Sivaganesan, S., Padma Sravya, N., & Parthiban, A. (2021) Experimental investigation on mechanical properties of carbon fiber reinforced aluminum metal matrix composite. *Materials Today: Proceedings*, 39, 743–747. <https://doi.org/https://doi.org/10.1016/j.matpr.2020.09.443>
- [16] Adeoti, M. O., Dahunsi, O. A., Awopetu, O. O., Aramide, F. O., Alabi, O. O., Johnson, O. T., & Abdulkarim, A. S. (2019) Suitability of selected Nigerian clays for foundry crucibles production, *Procedia Manufacturing*, 35, 1316–1323. <https://doi.org/10.1016/j.promfg.2019.05.023>
- [17] Fashu, S., Lototsky, M., Davids, M. W., Pickering, L., Linkov, V., Tai, S., ... Tarasov, B. P. (2019) A review on crucibles for induction melting of titanium alloys, *Materials & Design*, 186(108295), 1–17. <https://doi.org/10.1016/j.matdes.2019.108295>

- [18] Siddiqua, A., Hahladakis, J., & Al-Attiya, W. A. K. A. (2022) An overview of the environmental pollution and health effects associated with waste landfilling and open dumping, *Environmental Science and Pollution Research*, 29:58514–58536. <https://doi.org/10.1007/s11356-022-21578-z>
- [19] Department of Economic and Social Affairs, S. D. (2023), THE 17 GOALS | Sustainable Development. <https://sdgs.un.org/goals>
- [20] Singh, R. P., Reddy, P. S., Vanapalli, K. R., & Mohanty, B. (2023) Influence of binder materials and alkali activator on the strength and durability properties of geopolymer concrete: A review, *Materials Today: Proceedings*. 1–7. <https://doi.org/10.1016/j.matpr.2023.05.226>
- [21] Bagaiskov, Y. S., Krukhmaleva, G. P., & Shapovalova, M. P. (1989) Properties of the graphite-containing refractory crucibles based on a clay-kaolin binder, *Refractories*, 30(7), 475–478. <https://doi.org/10.1007/BF01280682>
- [22] Abdul Latif, Rusiyanto Rusiyanto, Sunyoto Sunyoto, Kriswanto Kriswanto, Deni Fajar Fitriyana (2022) Effect of Firing Temperature on Density, Porosity, Impact Strength, and Macro Structure of Crucible Materials Made from Graphite, Kaolin, and Castable Cement. *International Journal of Mechanical Engineering Technologies and Applications (MECHTA)*, 3(2), 93–99. <https://doi.org/10.21776/MECHTA.2022.003.02.3>
- [23] Ubani, A. C., & Atanmo, P. N. (2021) Effect of Granite, Kaolin Clay, Borosilicate Glass and Silicon Carbide in the Production of Graphite Crucibles, *International Journal of Engineering Research & Technology (IJERT)*, 10(12), 51–56. <https://www.ijert.org/effect-of-granite-kaolin-clay-borosilicate-glass-and-silicon-carbide-in-the-production-of-graphite-crucibles>
- [24] Popov, V., Fleisher, A., Muller-Kamskii, G., Avraham, S., Shishkin, A., Katz-Demyanetz, A., Travitzky, N., Yacobi, Y., & Goel, S. (2021) Novel hybrid method to additively manufacture denser graphite structures using Binder Jetting, *Scientific Reports*, 11(2438), 1–11. <https://doi.org/10.1038/s41598-021-81861-w>
- [25] Mukherjee, S., Das, S., Jain, A., & Ghosh, P. (2021) Oxidation protective coating of Y2O3-Na2Si6O13+1 composite on graphite crucible for high temperature applications, *Surfaces and Interfaces*, 25(101158), 1–10. <https://doi.org/10.1016/j.surf.2021.101158>
- [26] Palmonari, A., Cavallini, D., Sniffen, C. J., Fernandes, L., Holder, P., Fagioli, L., Fusaro, I., Biagi, G., Formigoni, A., & Mammi, L. (2020) Short communication: Characterization of molasses chemical composition, *Journal of Dairy Science*, 103(7), 6244–6249. <https://doi.org/10.3168/jds.2019-17644>
- [27] Şahinöz, M., Aruntaş, H. Y., & Gürü, M. (2022) Processing of polymer wood composite material from pine cone and the binder of phenol formaldehyde/PVAc/molasses and improvement of its properties. *Case Studies in Construction Materials*, 16(e01013), 1–15. <https://doi.org/10.1016/j.cscm.2022.e01013>
- [28] Kotta, A. B., Patra, A., Kumar, M., & Karak, S. K. (2019) Effect of molasses binder on the physical and mechanical properties of iron ore pellets. *International Journal of Minerals, Metallurgy and Materials*, 26(1), 41–51. <https://doi.org/10.1007/s12613-019-1708-x>
- [29] S. Bhide, Jayesh Darshane, D. Shinde, Sudhanshu Dhokale, P. Deshmukh, Yash desai, P. K. (2017). Effect of Sugarcane Molasses on Compressive Strength and Workability of Fly Ash Mixed Concrete. *International Journal of Scientific Research in Science, Engineering and Technology*, 3, 607–612. <https://www.researchgate.net/publication/328771482>
- [30] Wang, T., Wang, Z., Zhai, Y., Li, S., Liu, X., Wang, B., Li, C., & Zhu, Y. (2019) Effect of molasses binder on the pelletization of food waste hydrochar for enhanced biofuel pellets production, *Sustainable Chemistry and Pharmacy*, 14(100183), 1–8. <https://doi.org/10.1016/j.scp.2019.100183>
- [31] Olatunji, K. J., Idowu, K. E., & Dahiru, S. A. (2020) Industrial Potential and the Suitability of Emu-Agbaja, Oworo Clay for the Production of Refractory Bricks, *World Journal of Innovative Research*, 5, 122–129. [https://www.wjir.org/download\\_data/WJIR0905034.pdf](https://www.wjir.org/download_data/WJIR0905034.pdf)
- [32] Najafpour, G. D., & Poi Shan, C. (2003) Enzymatic hydrolysis of molasses, *Bioresource Technology*, 86(1), 91–94. [https://doi.org/10.1016/S0960-8524\(02\)00103-7](https://doi.org/10.1016/S0960-8524(02)00103-7)
- [33] Mohd Yatim, A. F., Syafiq, I. M., Huong, K. H., Abdullah Amirul, A. A., Mohd Effendy, A. W., & Bhubalan, K. (2017) Bioconversion of novel and renewable agro-industry by-products into a biodegradable poly(3-hydroxybutyrate) by marine *Bacillus megaterium* UMTKB-1 strain, *Biotechnology*, 98(2), 141–151. <https://doi.org/10.5114/bta.2017.68313>
- [34] Hassan, S. H. A., el Nasser A. Zohri, A., & Kassim, R. M. F. (2019) Electricity generation from sugarcane molasses using microbial fuel cell technologies, *Energy*, 178, 538–543. <https://doi.org/10.1016/j.energy.2019.04.087>
- [35] Jamir, L., Kumar, V., Kaur, J., Kumar, S., & Singh, H. (2021) Composition, valorization and therapeutical potential of molasses: a critical review, *Environmental Technology Reviews*, 10(1), 131–142. <https://doi.org/10.1080/21622515.2021.1892203>
- [36] Benkun Qi, Jianquan Luo, and Wan Yinhua (2018). Chemical Conversion of Molasses for Production of Levulinic Acid and Hydroxymethylfurfural. *Research and Advances: Environmental Sciences*, 1(1), 22–26. <https://doi.org/10.33513/raes/1801-06>

- [37] Callister, W. D., & Rethwisch, D. G. (2020) Fundamentals of materials science and engineering: an integrated approach 5<sup>th</sup> edition. Wiley, United States of America.
- [38] Irawan, A. P., Fitriyana, D. F., Siregar, J. P., Cionita, T., Anggarina, P. T., Utama, D. W., Rihayat, T., Rusiyanto, R., Dimiyati, S., Aripin, M. B., Ismail, R., Bayuseno, A. P., Baskara, G. D., Khafidh, M., Putera, F. P., & Yotenka, R. (2023) Influence of Varying Concentrations of Epoxy, Rice Husk, Al<sub>2</sub>O<sub>3</sub>, and Fe<sub>2</sub>O<sub>3</sub> on the Properties of Brake Friction Materials Prepared Using Hand Layup Method, *Polymers*, 15(2597), 1–19. <https://doi.org/10.3390/polym15122597>
- [39] Ismail, R., Cionita, T., Shing, W. L., Fitriyana, D. F., Siregar, J. P., Bayuseno, A. P., Nugraha, F. W., Muhamadin, R. C., Junid, R., & Endot, N. A. (2022) Synthesis and Characterization of Calcium Carbonate Obtained from Green Mussel and Crab Shells as a Biomaterials Candidate, *Materials*, 15(16), 1–15. <https://doi.org/10.3390/ma15165712>
- [40] Rusiyanto, R., Widodo, R. D., Al-Janani, D. H., Rohmah, K., Parlaungan Siregar, J., Nugroho, A., & Fitriyana, D. F. (2021) Effect of Sintering Temperature on the Physical Properties of Ba<sub>0.6</sub>Sr<sub>0.4</sub>TiO<sub>3</sub> Prepared by Solid-State Reaction, *International Journal of Automotive and Mechanical Engineering*, 18(2), 8752 – 8759. <https://doi.org/10.15282/ijame.18.2.2021.13.0669>
- [41] Qi, L., Han, T., & Zhang, Y. (2019). Electrostatic precipitability of TiB<sub>2</sub>-Fe-Mo-Co ceramic-metal composites. *Journal of Alloys and Compounds*, 778, 507–513. <https://doi.org/https://doi.org/10.1016/j.jallcom.2018.11.217>
- [42] Popov, O., Shtansky, D. V., Vishnyakov, V., Klepko, O., Polishchuk, S., Kutzhanov, M. K., Permyakova, E. S., & Teselko, P. (2022) Reaction Sintering of Machinable TiB<sub>2</sub>-BN-C Ceramics with In-Situ Formed h-BN Nanostructure, *Nanomaterials*, 12(8), 1–15. <https://doi.org/10.3390/NANO12081379>
- [43] Nguyen, T. P., Dashti Geremi, M., Hamidzadeh Mahaseni, Z., Delbari, S. A., Le, Q. Van, Ahmadi, Z., Shokouhimehr, M., Sabahi Namini, A., & Shahedi Asl, M. (2020) Enhanced densification of spark plasma sintered TiB<sub>2</sub> ceramics with low content AlN additive, *Ceramics International*, 46(14), 22127–22133. <https://doi.org/10.1016/j.ceramint.2020.05.278>
- [44] Ahmadi, Z., Mahaseni, Z. H., Geremi, M. D., & Asl, M. S. (2019) Microstructure of spark plasma sintered TiB<sub>2</sub> and TiB<sub>2</sub>-AlN ceramics, *Advanced Ceramics Progress*, 5(1), 36–40. <https://doi.org/10.30501/acp.2019.93129>
- [45] Shayesteh, F., Delbari, S. A., Ahmadi, Z., Shokouhimehr, M., & Shahedi Asl, M. (2019) Influence of TiN dopant on microstructure of TiB<sub>2</sub> ceramic sintered by spark plasma, *Ceramics International*, 45(5), 5306–5311. <https://doi.org/10.1016/j.ceramint.2018.11.228>
- [46] Shaddel, S., Sabahi Namini, A., Pazhouhanfar, Y., Delbari, S. A., Fattahi, M., & Shahedi Asl, M. (2020) A microstructural approach to the chemical reactions during the spark plasma sintering of novel TiC-BN ceramics, *Ceramics International*, 46(10), 15982–15990. <https://doi.org/10.1016/j.ceramint.2020.03.148>
- [47] Pourmohammadi Vafa, N., Ghassemi Kakroudi, M., & Shahedi Asl, M. (2020) Role of h-BN content on microstructure and mechanical properties of hot-pressed ZrB<sub>2</sub>-SiC composites, *Ceramics International*, 46(13), 21533–21541. <https://doi.org/10.1016/j.ceramint.2020.05.255>
- [48] Zhai, Y., Wang, T., Zhu, Y., Peng, C., Wang, B., Li, X., Li, C., & Zeng, G. (2018) Production of fuel pellets via hydrothermal carbonization of food waste using molasses as a binder, *Waste Management*, 77, 185–194. <https://doi.org/10.1016/j.wasman.2018.05.022>
- [49] Hamzah, M. S., Wildan, M. W., Kusmono, & Suharyadi, E. (2023) Effect of sintering temperature on physical, mechanical, and electrical properties of nano silica particles synthesized from Indonesia local sand for piezoelectric application, *Journal of Asian Ceramic Societies*, 11(1), 178–187. <https://doi.org/10.1080/21870764.2023.2173851>
- [50] Yu, W., Wang, J., Wu, Y., Zou, Z., Yu, Q., & Mo, P. (2017) In situ synthesis of polycrystalline cubic boron nitride with high mechanical properties using rod-shaped TiB<sub>2</sub> crystals as the binder, *Advances in Applied Ceramics*, 116(8), 419–427. <https://doi.org/10.1080/17436753.2017.1343781>
- [51] Tong, Q., Zhou, Y., Zhang, J., Wang, J., Li, M., & Li, Z. (2008) Preparation and properties of machinable Si<sub>2</sub>N<sub>2</sub>O/BN Composites, *International Journal of Applied Ceramic Technology*, 5(3), 295–304. <https://doi.org/10.1111/j.1744-7402.2008.02197.x>
- [52] Dey, D., Bal, K. S., Khan, I., Bangia, I., Singh, A. K., & Roy Choudhury, A. (2022) Study of tribo-mechanical properties of laser clad Al<sub>2</sub>O<sub>3</sub>-TiB<sub>2</sub>-TiN-BN||Ti-6Al-4 V alloy, *Optics & Laser Technology*, 150(107982), 1–18. <https://doi.org/10.1016/j.optlastec.2022.107982>
- [53] Ezéchiél, K., Joel, T. K., Abdon, A., & Roger, D. D. (2022). Accessibility and effects of binder types on the physical and energetic properties of ecological coal. *Heliyon*, 8(11), 1–7. <https://doi.org/10.1016/j.heliyon.2022.e11410>
- [54] Utchariyajit, K., Panprasert, V., Chayawat, L., Jungthanasombat, W., Janprom, P., & Choatchuang, M. (2019), Physical properties and calorific value of briquettes produced from Palmyra palm waste with molasses binder, *IOP Conference Series: Materials Science and Engineering*, 639(012046), 1–5. <https://doi.org/10.1088/1757-899X/639/1/012046>

- [55] Tanui, J. K., Kioni, P. N., Kariuki, P. N., & Ngugi, J. M. (2018) Influence of processing conditions on the quality of briquettes produced by recycling charcoal dust, *International Journal of Energy and Environmental Engineering*, 9(3), 341–350. <https://doi.org/10.1007/s40095-018-0275-7>
- [56] Carnaje, N. P., Talagon, R. B., Peralta, J. P., Shah, K., & Paz-Ferreiro, J. (2018) Development and characterisation of charcoal briquettes from water hyacinth (*Eichhornia crassipes*)-molasses blend, *PLoS ONE*, 13(11), 1–14. <https://doi.org/10.1371/journal.pone.0207135>
- [57] Crouter, A., & Briens, L. (2014) The effect of moisture on the flowability of pharmaceutical excipients, *AAPS PharmSciTech*, 15(1), 65–74. <https://doi.org/10.1208/s12249-013-0036-0>
- [58] Deshannavar, U. B., Hegde, P. G., Dhalayat, Z., Patil, V., & Gavas, S. (2018) Production and characterization of agro-based briquettes and estimation of calorific value by regression analysis: An energy application, *Materials Science for Energy Technologies*, 1(2), 175–181. <https://doi.org/10.1016/j.mset.2018.07.003>
- [59] Syahfitri, A., Hermawan, D., Kusumah, S. S., Ismadi, Lubis, M. A. R., Widyaningrum, B. A., Ismayati, M., Amanda, P., Ningrum, R. S., & Sutiawan, J. (2022) Conversion of agro-industrial wastes of sorghum bagasse and molasses into lightweight roof tile composite, *Biomass Conversion and Biorefinery*, 1–15. <https://doi.org/10.1007/s13399-022-02435-y>
- [60] Jiménez, J. E., Fontes Vieira, C. M., & Colorado, H. A. (2022) Composite Soil Made of Rubber Fibers from Waste Tires, Blended Sugar Cane Molasses, and Kaolin Clay, *Sustainability (Switzerland)*, 14(4), 1–15. <https://doi.org/10.3390/su14042239>
- [61] Thapa, P., Tripathi, J., & Jeong, S. H. (2019) Recent trends and future perspective of pharmaceutical wet granulation for better process understanding and product development, *Powder Technology*, 344, 864–882. <https://doi.org/10.1016/j.powtec.2018.12.080>
- [62] Khan, A. (2021), Prediction of quality attributes (mechanical strength, disintegration behavior and drug release) of tablets on the basis of characteristics of granules prepared by high shear wet granulation, *PLOS ONE*, 16(12), 1–19. <https://doi.org/10.1371/journal.pone.0261051>
- [63] Mohanty, D. D. (2011) Effect of Holding Time on Binder Burnout, Density and Strength of Green and Sintered Alumina Samples. [Master Thesis, National Institute of Technology Rourkela], Rourkela, India <https://core.ac.uk/download/pdf/53187944.pdf>
- [64] Liu, Y., Ma, L., Dong, R., Cui, K., Hou, Y., Yang, W., Liu, Y., Zhong, C., Wen, G., & Zhang, L. (2022) Binary Binder for Cf/C-SiC Composites with Enhanced Mechanical Property, *Materials (Basel, Switzerland)*, 15(2757), 1–14. <https://doi.org/10.3390/ma15082757>
- [65] Yu, J., Wang, H., Zhang, J., Zhang, D., & Yan, Y. (2010) Gelcasting preparation of porous silicon nitride ceramics by adjusting the content of monomers, *Journal of Sol-Gel Science and Technology*, 53(3), 515–523. <https://doi.org/10.1007/s10971-009-2125-9>
- [66] Ayorinde, J. O., Itiola, A. O., & Odeniyi, M. A. (2013) Effects of excipients and formulation types on compressional properties of diclofenac, *Acta Poloniae Pharmaceutica - Drug Research*, 70(3), 557–566. [https://www.ptfarm.pl/pub/File/Acta\\_Poloniae/2013/3/557.pdf](https://www.ptfarm.pl/pub/File/Acta_Poloniae/2013/3/557.pdf)
- [67] Babapoor, A., Asl, M. S., Ahmadi, Z., & Namini, A. S. (2018) Effects of spark plasma sintering temperature on densification, hardness and thermal conductivity of titanium carbide, *Ceramics International*, 44(12), 14541–14546. <https://doi.org/10.1016/j.ceramint.2018.05.071>
- [68] Kamal Jayaraj, R., Malarvizhi, S., & Balasubramanian, V. (2017) Optimizing the micro-arc oxidation (MAO) parameters to attain coatings with minimum porosity and maximum hardness on the friction stir welded AA6061 aluminium alloy welds, *Defence Technology*, 13(2), 111–117. <https://doi.org/10.1016/j.dt.2017.03.003>
- [69] Cherry, J. A., Davies, H. M., Mehmood, S., Lavery, N. P., Brown, S. G. R., & Siensz, J. (2015) Investigation into the effect of process parameters on microstructural and physical properties of 316L stainless steel parts by selective laser melting, *International Journal of Advanced Manufacturing Technology*, 76(5–8), 869–879. <https://doi.org/10.1007/s00170-014-6297-2>
- [70] S. Kumar Singh, A. Kumar, and A. Jain (2018) Improving tensile and flexural properties of SiO<sub>2</sub>-epoxy polymer nanocomposite, *Materials Today: Proceedings*, 5(2), 6339–6344, <https://doi.org/10.1016/j.matpr.2017.12.243>
- [71] Fitriyana, D. F., Nugraha, F. W., Laroybafih, M. B., Ismail, R., Bayuseno, A. P., Muhamadin, R. C., Ramadan, M. B., Qudus, A. R. A., & Siregar, J. P. (2022) The effect of hydroxyapatite concentration on the mechanical properties and degradation rate of biocomposite for biomedical applications, *IOP Conference Series: Earth and Environmental Science*, 969(1), 1–8. <https://doi.org/10.1088/1755-1315/969/1/012045>
- [72] Ismail, R., Cionita, T., Lai, Y. L., Fitriyana, D. F., Siregar, J. P., Bayuseno, A. P., Nugraha, F. W., Muhamadin, R. C., Irawan, A. P., & Hadi, A. E. (2022), Characterization of PLA/PCL/Green Mussel Shells Hydroxyapatite (HA) Biocomposites Prepared by Chemical Blending Methods, *Materials*, 15(23), 1–18. <https://doi.org/10.3390/ma15238641>

- [73] Shivakumar, K. N., Brown, W. H., & Imran, K. A. (2019) Fly Ash Composites, A Step toward Pond Ash Composites, *Coal Combustion and Gasification Products 11 (2)*: 66–74. <https://doi.org/10.4177/CCGP-D-18-00014.1>
- [74] Laoubi, H., Bederina, M., Djoudi, A., Goullieux, A., Dheilly, R. M., & Queneudec, M. (2018) Study of a New Plaster Composite Based on Dune Sand and Expanded Polystyrene as Aggregates. *The Open Civil Engineering Journal*, 12(1), 401–412. <https://doi.org/10.2174/1874149501812010401>
- [75] Filipčev, B., Šimurina, O., Dapčević Hadnađev, T., Jevtić-Mučibabić, R., Filipović, V., & Lončar, B. (2015) Effect of Liquid (Native) and Dry Molasses Originating from Sugar Beet on Physical and Textural Properties of Gluten-Free Biscuit and Biscuit Dough, *Journal of Texture Studies*, 46(5), 353–364. doi:10.1111/jtxs.12135
- [76] Lv, C., Ren, X., Wang, C., & Peng, Z. (2020) Spark plasma sintering of ultrafine WC-10Ni-ZrC hardmetals: Effects of adding ZrC nano-powder, *International Journal of Applied Ceramic Technology*, 17(3), 932–940. <https://doi.org/10.1111/ijac.13475>
- [77] Liu, Z., Zhao, S., Yang, T., & Zhou, J. (2021) Improvement in mechanical properties in AlN-h-BN composites with high thermal conductivity, *Journal of Advanced Ceramics*, 10(6), 1317–1325. <https://doi.org/10.1007/s40145-021-0506-0>
- [78] NC Elements. LLC. (2019). Boron nitride crucible. [https://ncelements.com/all\\_products/boron-nitride-crucible/](https://ncelements.com/all_products/boron-nitride-crucible/)
- [79] MTI Korea. (2022). Graphite-crucible. <https://mtikorea.co.kr/product/graphite-crucible-1quotod-x-059quotid-x-375quotdp-eq-g25100-ld/3847/>
- [80] Hoseinpur, A., & Safarian, J. (2020) Mechanisms of graphite crucible degradation in contact with Si–Al melts at high temperatures and vacuum conditions, *Vacuum*, 171, 1–12. <https://doi.org/10.1016/j.vacuum.2019.108993>
- [81] Shanghai Kessen Ceramics Co. Ltd. (2022). White Zirconia Crucible Technical Parameter. <https://d1c6gk3tn6ydje.cloudfront.net/1475960814803394560%2F8d69607ac5c8d4ecbe991c16c9191ba5.pdf>
- [82] Songhan Plastic Technology Co.Ltd. (2023, June 12). Crucible Steel SIL 1 (JIS SUH1) Martensitic Steel. <http://www.lookpolymers.com/pdf/Crucible-Steel-SIL-1-JIS-SUH1-Martensitic-Steel.pdf>
- [83] Materials, A. C. (2023). Aluminum Oxide Crucible. <https://www.preciseceramic.com/products/alumina-crucible.html>